Lasers in Medical Science (2019) 34:667–675
https://doi.org/10.1007/s10103-018-2638-y

ORIGINAL ARTICLE

Effect of photobiomodulation on neural differentiation of human umbilical cord mesenchymal stem cells

Hongli Chen[1,2] · Hongjun Wu[1] · Huijuan Yin[2] · Jinhai Wang[1] · Huajiang Dong[3] · Qianqian Chen[2] · Yingxin Li[2]

Received: 24 July 2018 / Accepted: 11 September 2018 / Published online: 19 September 2018

Abstract

Photobiomodulation therapy (PBMT) can enhance the mesenchymal stem cell (MSC) proliferation, differentiation, and tissue repair and can therefore be used in regenerative medicine. The objective of this study is to investigate the effects of photobiomodulation on the directional neural differentiation of human umbilical cord mesenchymal stem cells (hUC-MSCs) and provide a theoretical basis for neurogenesis. hUC-MSCs were divided into control, inducer, laser, and lasers combined with inducer groups. A 635-nm laser and an 808-nm laser delivering energy densities from 0 to 10 J/cm^2 were used in the study. Normal cerebrospinal fluid (CSF) and injured cerebrospinal fluid (iCSF) were used as inducers. The groups were continuously induced for 3 days. Cellular proliferation was evaluated using MTT. The marker proteins nestin (marker protein of the neural precursor cells), NeuN (marker protein of neuron), and GFAP (glial fibrillary acidic protein, marker proteins of glial cells) were detected by immunofluorescence and western blot. We found that irradiation with 635-nm laser increased cell proliferation, and that with 808 nm laser by itself and combined with cerebrospinal fluid treatment generated significant neuron-like morphological changes in the cells at 72 h. Nestin showed high positive expression at 24 h in the 808 nm group. The expression of GFAP increased in the 808-nm combined inducer group at 24 h but decreased at 72 h. The expression of neuN protein increased only at 72 h in both the 808-nm combined inducer group and inducer group. We concluded that 808 nm laser irradiation could help CSF to induce neuronal differentiation of hUC-MSCs in early stage and tend to change to neuron rather than glial cells.

Keywords Low-level laser · Photobiomodulation · Mesenchymal stem cells · Cerebrospinal fluid · Neural differentiation

Introduction

Stem cells are referred to as "universal cells" and have the potential to differentiate into multiple lineages. They possess proliferation and self-renewal properties. Two kinds of stem cells exist—embryonic stem cells (ES) and adult stem cells. Bone marrow, fat, placenta, cord blood, and umbilical cord are common sources of adult stem cells [1]. In recent years, stem cell therapy has received extensive attention and recognition in regenerative medicine. Clinical research has mainly focused on heart disease, retinal diseases, diabetes, and neurological diseases [2, 3]. Many studies have found that mesenchymal stem cells (MSCs) can be used in the treatment of neurological diseases including spinal cord injury, Alzheimer's disease, and stroke [4, 5]. Autologous immune rejection after stem cell transplantation makes the therapeutic effect unsatisfactory, making stem cell therapy in the clinic challenging [6]. In addition, the differentiation of MSCs is multi-directional and is regulated by many factors in vivo. The lack of guidance and regulation leads to uncontrolled proliferation and may promote tumor formation [7, 8]. Therefore, there are many safety concerns in the use of stem cells for treatment. To address these safety concerns, it is important to understand the process of induction of differentiation in stem cells and the mechanisms of stem cell differentiation.

The umbilical cord is an easily accessible source of adult stem cells. Human umbilical cord mesenchymal stem cells (hUC-MSCs) are highly purified and have a strong paracrine function.

✉ Huijuan Yin
yinzi490@163.com

✉ Jinhai Wang
wangjinhai@tjpu.edu.cn

[1] School of Electronics and Information Engineering, Tianjin Polytechnic University, Tianjin 300387, China

[2] Laboratory of Laser Medicine, Institute of Biomedical Engineering, Chinese Academy of Medical Sciences & Peking Union Medical College, Tianjin 300192, China

[3] Logistics University of People's Armed Police Force, Tianjin 300309, China

The use of hUC-MSCs for scientific studies is regarded ethical [9]. hUC-MSC differentiation into neural cell follows two phases—an induction phase and a differentiation phase. At present, there are many methods for inducing hUC-MSCs into neural cells in vitro. In the pre-induction phase, the neural stem cells (NSCs) are dependent on the synergistic promotion of nutritional factors [10]. Brain-derived neurotrophic factor (BDNF), epidermal growth factor (EGF), basic fibroblast growth factor (bFGF), and other nutritional factors are often used to trigger this phase [11–13]. Robinson J [14] found that vascular endothelial growth factor (VEGF), BDNF, and bFGF were important for the differentiation of neural stem cells by comparative analysis of different neurotrophic factors. Middle cerebral artery occlusion (MCAO) mouse experiment also proved that bFGF played a key role in the differentiation process of neural stem cells [12, 15]. Neurotrophic factors can specifically bind to the surface receptors of MSCs and promote cell differentiation and can also regulate cell microenvironment and increase cell viability. In the second stage, NSCs differentiate into specific cells, such as neurons, glial cells, and oligodendrocytes. The induction strategy at this stage mainly includes the use of chemical inducers and nutrition factors. Co-culture method is another common procedure [16]. Compared to the nutrient factors, β-sulfhydryl ethanol, dimethyl sulfoxide (DMSO), retinoic acid (RA), and other chemical inducers have higher efficiency but have adverse effects on cell viability [17]. At present, chemical inducers are considered unsafe and are used only for scientific research and not in the clinic.

The differentiated process of hUC-MSCs is more complex than NSCs. The study found that hUC-MSCs had high expression of nestin in the early induction [5], which is an intermediate filament protein distributed around the cytoplasm. NSCs often use this protein as a specific marker, but their expression is transient and not easy to detect. Neural stem cells may develop to many types of terminal neural cells, such as neurons and glial cells. The different induction goal needs different induction condition. Cui YB [9] stained the pathological sections of transplanted stem cells in the hippocampus and found that neuN (mature neurons) was highly positively expressed, and the mice restored hippocampal neurogenesis. Zhang JJ [11] transplanted NSCs combined with bFGF to MCAO and found the expression of GFAP (astrocytes) and neuN increasing, which indicated that NSCs achieve differentiation into neurons and glial cells. Robinson J also further proved this conclusion [14]. From the above, nestin, neuN, and GFAP were regarded as the marker of neural precursor cells, mature neurons, and astrocytes, respectively.

With the development of laser medicine, photobiomodulation has become an intensively studied subject [18]. Low-level laser therapy (LLLT) or photobiomodulation therapy (PBMT) refers to the use of low-energy lasers to induce changes in the immune system, blood circulation system, and tissue metabolism [18] and is safer, more reliable, and has fewer side effects. This treatment does not cause irreversible tissue damages and is widely used in clinical practice to relieve pain, repair wounds, and reduce inflammation [19]. PBMT has important research significance and application prospect in regenerative medicine. Studies have found that light-emitting diode (LED) irradiation can eliminate amyloid proteins in a mouse model of Alzheimer's disease, which strongly proved that photobiomodulation has a regulatory effect on neurological diseases [20]. Cerebrospinal fluid (CSF), an important microenvironment component of human brain cells, contains a variety of nutrients required for neurons [21].

In this study, we used semiconductor lasers combined with inducers to differentiate hUC-MSCs into nerve cells and increase their activity. We attempted to assess neural differentiation of stem cells by protein detection (nestin, neuN, and GFAP).

Materials and methods

Isolation and expansion of hUC-MSCs

Umbilical cords (UCs) were obtained from healthy donors at the First Central Hospital of Tianjin (Tianjin, China). All clinical procedures followed the protocols approved by the ethical committee. All participants provided their written consents for the current study. After collection, the cords were stored in 0.9% NaCl solution. The umbilical cord was washed in phosphate-buffered saline (PBS, TBD, China) and the umbilical vein (UCV), the umbilical arteries (UCAs), and mucous membrane tissues removed. The Wharton's jelly (WJ) was isolated, cut into 2–3 mm pieces, and centrifuged at 1923×*g* for 10 min at 22 °C. The pellet was incubated in PBS with 1 mg/ml collagenase type I for 4–5 h in 75 cm^2 culture dishes (Corning, NY) in a CO_2 incubator at 37 °C. After 4 h, the dishes were inverted and placed upside down overnight. Human mesenchymal stem cell serum-free basic medium supplemented with 10% human mesenchymal stem cell serum-free additives (TBD, China) was added to the dishes and continuously cultured for 12 days. When a sufficient number of cells crawled out of the tissue mass and began to fall off, they were digested with 0.25% trypsin-EDTA (Gibco), diluted and cultivated continuously in fresh medium.

Flow cytometric determination of hUC-MSC phenotype

The expanded second passage hUC-MSCs were digested and resuspended at a concentration of 1×10^6 cells/ml in PBS. The cells were incubated with the primary antibodies at 4 °C for 30 min. Anti-CD105-PE (phycoerythrin), anti-CD90-PerCP-Cyanine, and anti-CD73-FITC (fluorescein isothiocyanate) were used to identify MSCs. Anti-CD31-FITC was used as an endothelial cell marker, and anti-CD45-PerCP-Cyanine and anti-CD34-APC (allophycocyanin) were used as

hematopoietic cell markers. All antibodies were purchased from Wuhan Gene Create Biological Engineering Company (China). After incubation, the cells were washed twice to remove unbound antibodies and resuspended in 500 μL Cell Fix (BD Biosciences). Negative controls included unstained hUC-MSCs and stained hUC-MSCs incubated with isotype control antibodies. The cells were scanned using a FACSCanto II flow cytometer (BD Biosciences) and analyzed using FACSDiva version 6.1.1 software (BD Biosciences).

Observation of cell growth and cell morphology

hUC-MSCs were plated in 96-well plates at a density of 2×10^3 cells/well (0.1 mL) and cultured overnight. Cells were grouped into a control group and experimental groups. The experimental groups were irradiated with 635- and 808-nm lasers with a power density of 20 mW/cm^2 (Institute of biomedical engineering, Chinese Academy of medical sciences, China). The total energy densities delivered were 2 J/cm^2, 3 J/cm^2, 4 J/cm^2, 6 J/cm^2, 7 J/cm^2, 8 J/cm^2, and 10 J/cm^2. All parameters of the laser device were selected in Table 1. The experimental groups were irradiated once a day for 3 consecutive days. Cell viability was assayed at 24 h, 48 h, and 72 h after irradiation using 3-(4,5-dimethylthinazol-2-yl)-2,5-diphenyl tetrazolium bromide (MTT). The cells were washed twice with PBS and 100 μL MTT (0.5 mg/mL) was added to each well. The plates were incubated for 4 h in a humidified atmosphere at 37 °C with 5% CO_2. After incubation, 150 μL DMSO was added to each well and incubated for 15 min. The absorbance (490 nm) was read using a multi-function microplate reader (Thermol Fisher, USA). Cell morphology was studied using an inverted microscope (Olympus, Japan).

hUC-MSC differentiation

For monitoring MSC differentiation into neural-like cells, hUC-MSCs were plated in 24-well plates at a density of 1×10^5 cells/wells and cultured overnight. The cells were grouped into control group, inducer group, laser group, and combined inducer with laser group. Cerebrospinal fluid (CSF, Affiliated hospital of armed police logistics college, China) and injured cerebrospinal fluid (iCSF) were used as inducers. Induction time was 24 and 96 h. A 635-nm laser and an 808-nm laser with a power density of 20 mW/cm^2 delivering an energy density of 6 J/cm^2 were used for irradiation. The experimental groups were irradiated once a day for 3 consecutive days (Fig. 1a). The positive control groups were induced using neurotrophic growth factors—20 μg/L basic fibroblast growth factor (bFGF, Gibco) and epidermal growth factor (EGF, Gibco) in 1% DMSO.

Table 1 Irradiation parameters

Parameter [unit]	Value
Center wavelength [nm]	635/808
Output mode	Continue
Average radiant power [mW]	40
Spot area [cm^2]	2
Irradiance at aperture [mW/cm^2]	20
Beam profile	Round
Beam divergence [rad or deg]	90

Immunofluorescent characterization of hUC-MSC differentiation

For immunofluorescent staining, the cells were transferred to cell culture slides (Solarbio, China). To characterize the induced cells, they were fixed with 4% methanol for 10 m and non-specific protein interactions were blocked using 0.1% PBS-Tween buffer containing 1% BSA for 1 h at 37 °C. Subsequently, the cells were incubated with primary antibodies overnight at 4 °C. Primary antibodies included nestin (1:1000, Abcam, USA), NeuN (1:1000, Abcam, USA), and human GFAP (1:1000, Abcam, USA). The slides were washed with PBS (twice, 10 m each), and then incubated for 1 h with a secondary antibody against rabbit IgG conjugated with FITC (1:1000, Abcam, USA) at room temperature. The cells were washed with PBS (twice, 10 m each) and counterstained with DAPI (Solarbio, China) for 30 min at room temperature. The slides were washed with PBS (twice, 10 m each), mounted with anti-fluorescence quenching agent (Beyotime, China), and observed on an inverted fluorescent microscope (Zeiss LSM710, Germany).

Western blot analysis

To get sufficient amount of protein, hUC-MSCs were plated in 6-well plates at a density of 5×10^5 cells/well and cultured overnight. Every group had three samples. The supernatant was discarded. After washing twice with PBS, the induced cells were incubated on ice for 15 min with 1% PMSF-RIPA (Beyotime, China). All samples were centrifuged at 12,000×*g* for 5 min at 4 °C. The supernatant was used to determine nestin, NeuN, and GFAP (ZENBIO, China). The protein concentration was determined by the BCA assay (Solarbio, China). An equal amount of protein (50 μg/lane) was subjected to SDS-PAGE (Beyotime, China) and transferred to polyvinylidene fluoride membranes (PVDF, Beyotime, China). Blots were blocked for 2 h in 5% BSA (Solarbio, China)-TBS-0.1% Tween-20 and then washed with TBS-0.1% Tween-20 three times. The blots were incubated with the primary antibodies at 4 °C overnight, and then with a horseradish peroxidase-conjugated secondary anti-rabbit antibody (1:8000, ZENBIO, China) for 1 h. Immunoreactivity was detected using enhanced chemiluminescence detection reagents (BeyoECL Star, Beyotime, China) on a gel imaging system (Bio-Rad, USA).

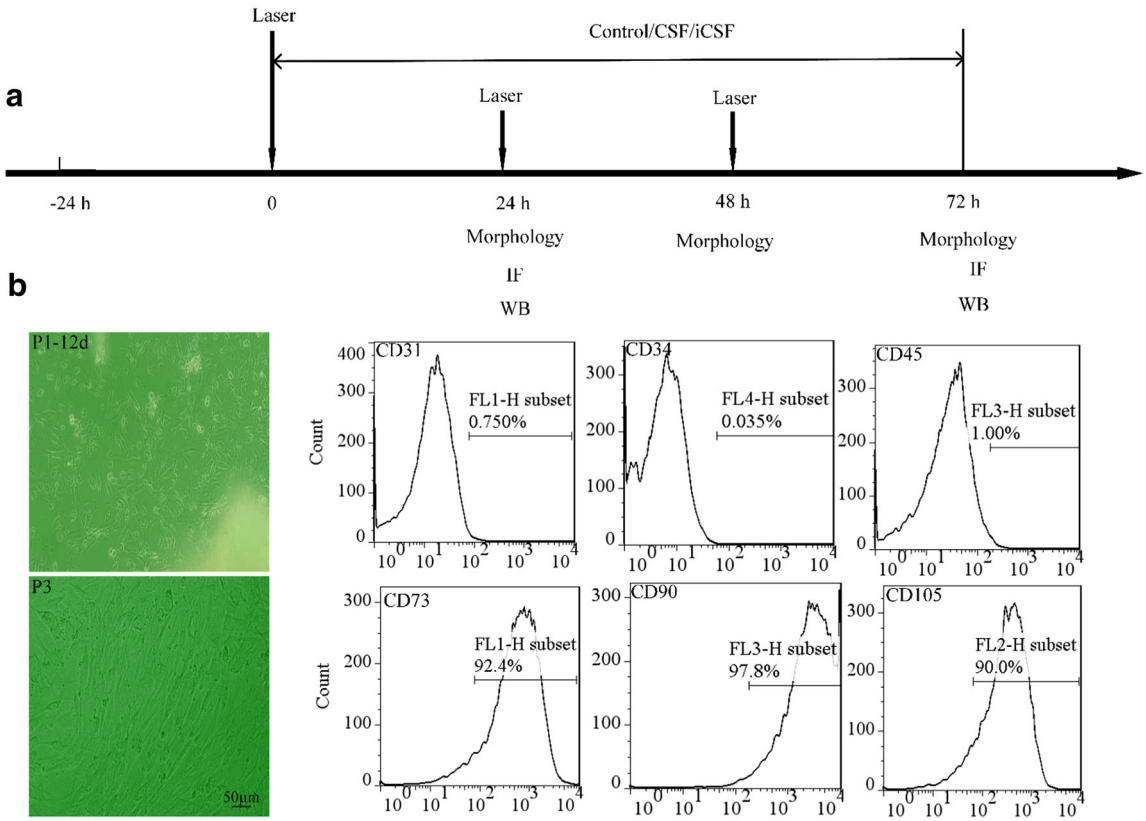

Fig. 1 HUC-MSCs detection and culture. **a** The route of induced differentiation of hUC-MSCs and detection. **b** Morphology of hUC-MSCs at 12 days and passion 3 (left) and identification of hUC-MSCs by flow cytometric evaluation of expression of cell surface markers (right)

Statistical analysis

All data are presented as mean ± standard deviation. The data were analyzed using one-way analysis of variance (ANOVA), followed by Student's two-tailed *t* test for comparison between two groups. $P < 0.05$ was considered significant.

Results

Morphologic observations

Morphologic observation of hUC-MSCs is the most intuitive method for clearly distinguishing cell types. At plating, the WJ covered the culture plates evenly. Some tissue began to fall off on day 10 of culture, and a small number of cells crawled out of the tissue mass. Figure 1b shows the MSCs on day 12 of culture. Primary cells crawled out along the edge of the tissue. The cells were short shuttle-like and very small. When the cells reached 80–90% confluence, they were digested with 0.25% trypsin-EDTA and passaged. At this stage, the cells proliferated at an accelerated rate and were spindle-shaped. Cells from passage 3 grew directionally and a fibroblast-like long spindle morphology was observed (Fig. 1b). A stable growth rate was observed during this phase. The proliferation rate dropped after passage six.

Immunophenotype analysis by flow cytometry

We investigated the immunophenotypes of the hUC-MSCs from passage 3 by flow cytometry. Ninety percent of cells expressed the MSC markers including CD73, CD90, and CD105 (Fig. 1b). Approximately 1% of cells expressed the markers for BMSCs including CD31, CD34, and CD45. Low CD31 and CD34 expressions suggested that the cells were not endothelial cells or blood cells. These results suggest that the cells were hUC-MSCs.

Effect of photobiomodulation on the proliferation of hUC-MSCs

hUC-MSC viability was detected by MTT assay. The 635-nm laser induction group showed significantly higher viability at 72 h compared to the control group. Higher cell numbers were observed in cells that received 2 J/cm^2, 3 J/cm^2, and 4 J/cm^2 energy densities (Fig. 2a). Treatment with CSF and iCSF inhibited the 635-nm laser-induced cell proliferation (Fig. 2c). No significant change in cell numbers was observed in the 808-nm laser induction group (Fig. 2b). CSF and iCSF treatments in the 808-nm laser induction group did not show any significant changes (Fig. 2d). This suggests that induction with 635 nm laser can promote cell proliferation in hUC-MSCs. Although

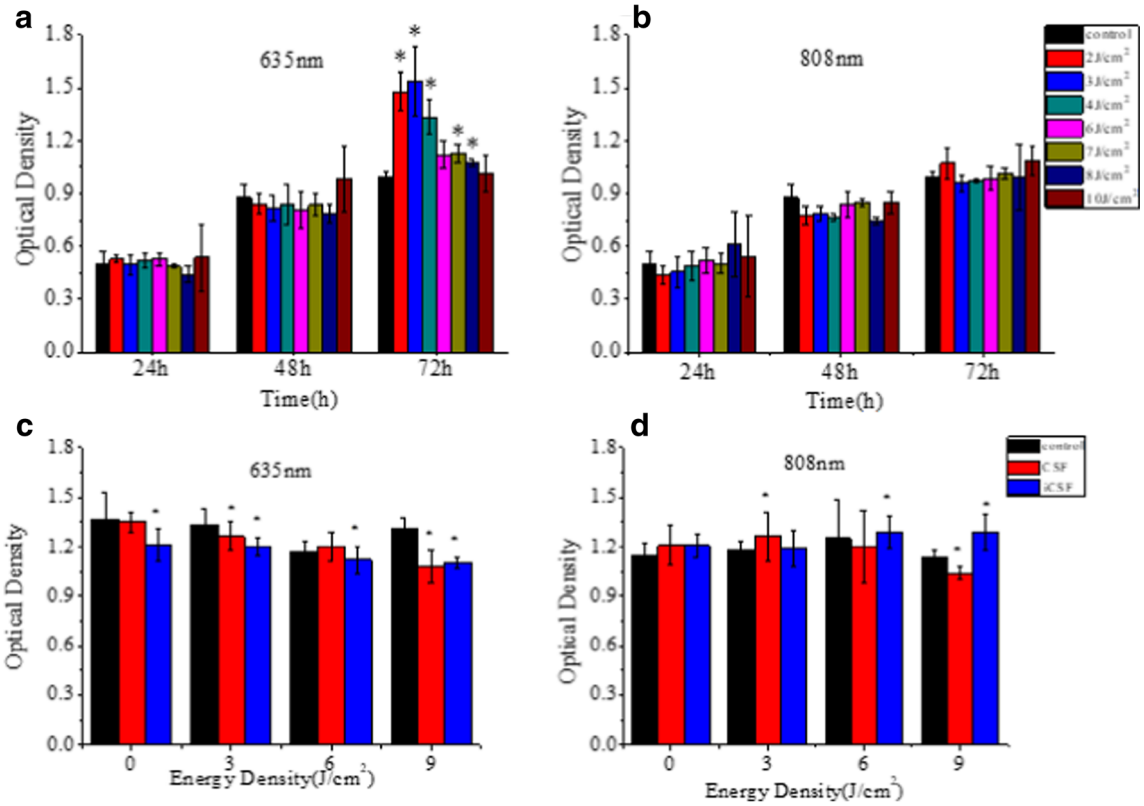

Fig. 2 Cell proliferation analysis. Cell viability of hUC-MSCs irradiated with **a** 635 nm laser and **b** 808 nm laser at different time points. Cell viability in cells treated with differentiation inducers CSF and iCSF and irradiated with **c** 635 nm laser and **d** 808 nm laser were tested by MTT at 72 h. Data presented as mean ± SD, $n = 3$ each group; $^*P < 0.05$

we did not find the significant proliferation of hUC-MSCs treated by 808-nm laser irradiation, the neural-like morphologic changes were observed as the followed results.

Morphologic changes in hUC-MSC treated with inducers

Cell morphology was observed at 24 h, 48 h, and 72 h after induction. At 24 h after induction, the control cells were directional and non-transparent and no significant increase in proliferation was observed in the experimental groups (Fig. 3a). The cells that received the induction treatment maintained their long spindle morphology. Morphological changes in the experimental group were observed at 48 h after induction (Fig. 3b). Cell densities in the experimental groups were lower than in the control group. The cells that received CSF were slenderer and formed meshes (indicated by arrows in Fig. 3b). A significant increase in cell proliferation was observed in the 635 nm laser induction group. A few cells had multiple branches. The 808-nm laser-induced cells formed triangle-shaped meshes with elongated vertices. This is a typical morphological characteristic of neurons in culture. The cell gap was smaller and the nuclei larger in the combined 808 nm laser—CSF group compared to the 808-nm laser alone group. At 72 h after induction, the cells overlap, and no clear space was observed between cells. In the experimental groups, a nest-like morphology was observed. A small amount of cell death was also observed (Fig. 3c).

Immunofluorescence identification of hUC-MSC differentiation

Expression of nerve cell markers including NeuN, GFAP, and nestin in the cells was studied by immunocytochemistry. Nestin is a major protein in neural stem cells. At 24 h after induction, the control and the CSF- and iCSF treated cells had low nestin expression. Most of the nestin in the CSF- and iCSF-treated cells was localized near the nucleus (Fig. 4a). Irradiation with lasers increased nestin expression. Nestin was localized in the cytoplasm and the cells were triangular in shape. Nestin expression in the 808-nm and 808-nm laser combined with the CSF groups was higher and the 808-nm laser group had the highest expression (Fig. 4c).

At 72 h after induction, the cells in the iCSF group were relatively slender (Fig. 4b). The 635-nm laser group had decreased nestin expression, while the 808-nm group showed enhanced nestin expression. The 808-nm laser-induced cells were slender and resembled long spindles. In the combined 635 nm laser-CSF group, enhanced nestin expression was observed, and most cells had a triangular morphology. The combined 808 nm

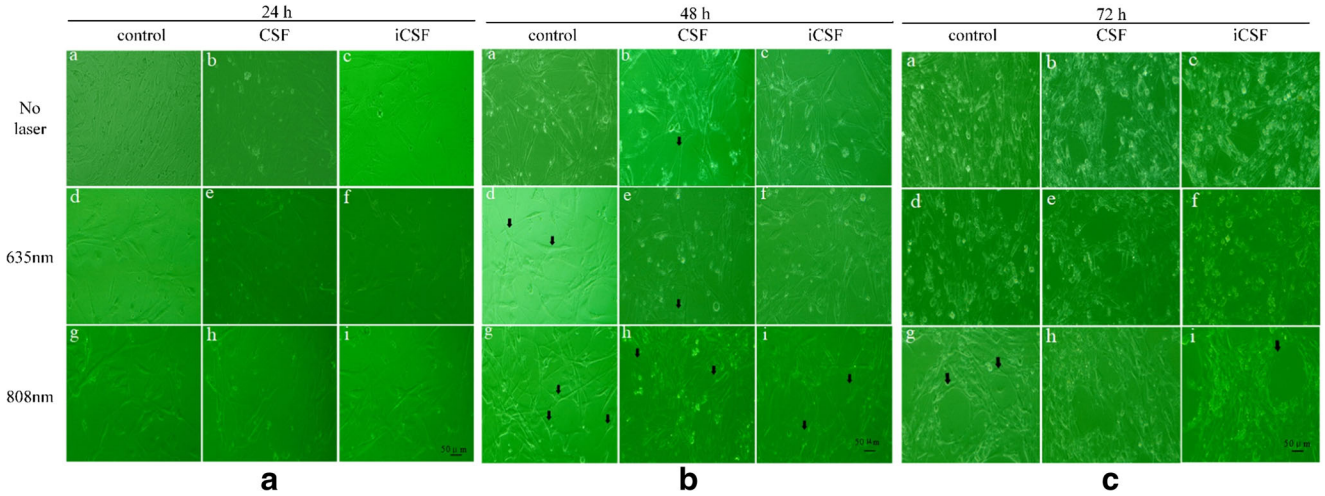

Fig. 3 Morphology of cells were observed by light microscopy after induction. **a** Morphology of cells at 24 h after induction (× 200). **b** Morphology of cells at 48 h after induction (× 200×). **c** Morphology of cells at 72 h after induction (× 200). Experimental groups included a control group, b CSF group, c iCSF group, d 635 nm laser group, e 635 nm laser combined with CSF group, f 635 nm laser combined with iCSF group, g 808 nm laser group, h 808 nm laser combined with CSF group, and i 808 nm laser combined with iCSF group

laser-CSF group also had increased expression of nestin and the cell growth showed a bipolar pattern. Cells treated with either of the lasers and iCSF had low nestin expression. These results suggest that the 808-nm laser was more effective than the 635-nm laser in promoting hUC-MSC differentiation into nerve cells. The results also demonstrate that CSF is a better inducer than iCSF. Nestin expression in the 635-nm combined with CSF group, the 808-nm laser group, and the 808-nm laser combined with the inducer group was higher, and the 808-nm laser group had the highest expression (Fig. 4c). GFAP and neuN proteins were not expressed at 72 h after induction (Fig. 4d, e).

Western blot analysis

The expression of GFAP, NeuN, and the internal reference protein glyceraldehyde-3-phosphate dehydrogenase (GAPDH) was

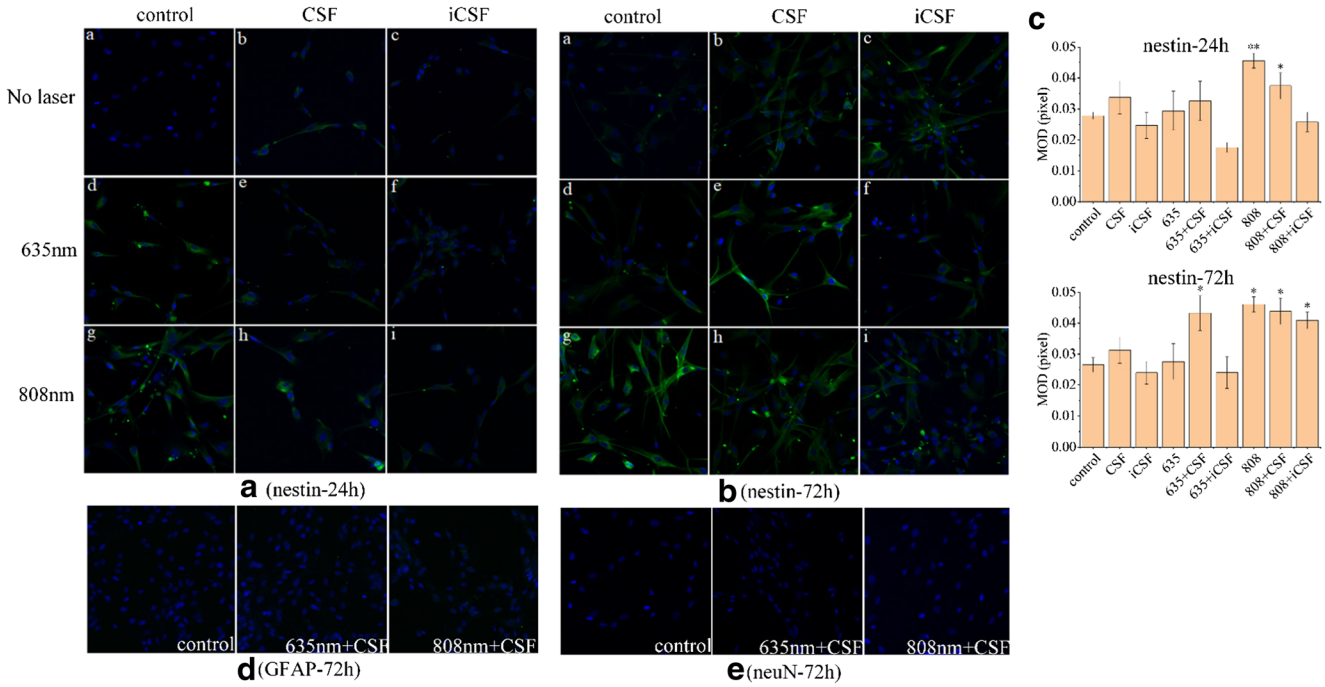

Fig. 4 Immunofluorescence analysis of GFAP, neuN, and nestin stained in green and nucleus stained by DAPI in blue were observed. **a** Nestin expression at 24 h and **b** 72 h after induction (× 200). **c** Mean optical density of nestin from **a** and **b** were calculated with histogram. **d** GFAP and **e** neuN expression at 72 h after induction (× 200). Data presented as mean ± SD, $n = 3$ each group; $^*P < 0.05$. Note: Experimental groups included a control group, b CSF group, c iCSF group, d 635 nm laser group, e 635 nm laser combined with CSF group, f 635 nm laser combined with iCSF group, g 808 nm laser group, h 808 nm laser combined with CSF group, and i 808 nm laser combined with iCSF group

assayed semi-quantitatively at 24 and 72 h after induction. GFAP expression in the cytoplasm is a marker of glial cells, and NeuN expression in the nucleus is a characteristic of nerve cells. At 24 h after induction, all cells expressed GFAP and the 808-nm laser combined treatment groups showed the highest expression (Fig. 5a). The expression was similar to that in the positive controls. Very little NeuN expression was observed in all cells at 24 h after induction. Densitometric analyses of the blots revealed that the expression of GFAP at 24 h after induction in the inducer groups was lower than that in positive control groups. GFAP expression in the 635- and 808-nm laser combined with the inducer groups was higher, and the 808-nm laser combined with the inducer group had the highest expression (Fig. 5b). The expression of NeuN in the iCSF group, 635 nm laser combined with inducer groups, and 808 nm laser group was lower than that in the control group. No change in expression was observed in the 808-nm laser combined with inducer groups and CSF group did (Fig. 5b).

No significant differences in GFAP expressed were observed at 72 h after induction ($P > 0.05$) (Fig. 5). Increased neuN expression was observed in the CSF group, the iCSF group, and the 808-nm laser combined inducer groups. The expression of neuN was high in the CSF group. Expression in the laser groups and lasers combined with inducer groups was higher than in the positive control. The combined 808 nm laser-iCSF group had the highest expression (Fig. 5b). These results suggest that the 808-nm laser combined with inducers could promote hUC-MSC differentiation into glial cells. The neuronal orientation was more pronounced when the hUC-MSCs were irradiated with an 808-nm laser combined with iCSF treatment.

Discussion

In this study, we discovered that lasers combined with iCSF could significantly increase the differentiation of hUC-MSCs into neural cells. Photobiomodulation has been widely studied in cell proliferation [22–24]. R. Fekrazad [24] found that red and near-infrared light with a wavelength in the range of 600–700 nm promotes MSC proliferation. We irradiated hUC-MSCs with a 635-nm and an 808-nm laser delivering different energy densities for three consecutive days and compared cell proliferation rates. We found that the 635 nm laser working at energy densities of 2 J/cm^2, 3 J/cm^2, and 4 J/cm^2 enhanced cell proliferation. In contrast, the 808 nm laser did not show any significant changes in cell proliferation. We also found that treatment with neural inducers CSF and iCSF inhibited the proliferation of hUC-MSCs irradiated with a 635-nm laser. This suggests that the dosage of inducers is very important for achieving optimal proliferation.

Very few studies have focused on the effects of photobiomodulation on the differentiation of stem cells into nerve cells. It is known that photobiomodulation has a dose-dependent effect on cell differentiation. Soleimani [25] found that 810-nm lasers promoted the differentiation of bone marrow stem cells (BMSCs) into neural cells at energy densities of 3 and 6 J/cm^2 and differentiation into osteoblasts at 2 and 4 J/cm^2. Peng [26] demonstrated that irradiation with a 620-nm light-emitting diodes (LEDs) combined with osteogenic inducer treatments promoted efficient osteogenic differentiation in BMSCs. These findings suggest that photobiomodulation combined with inducers has a positive effect on stem cell differentiation.

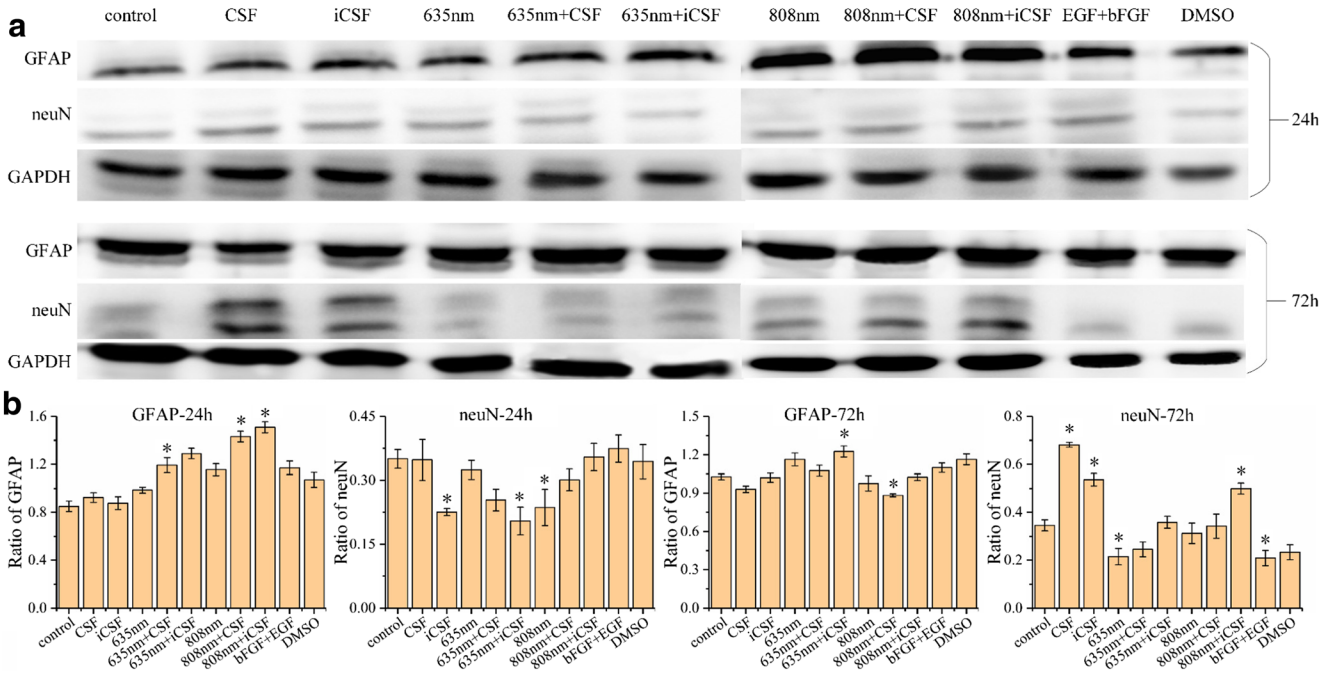

Fig. 5 Western blot analysis of GFAP, and neuN were tested at 24 and 72 h, and glyceraldehyde-3-phosphate dehydrogenase (GAPDH) as reference. **a** Protein expression of WB. **b** Semi-quantitative densitometric analysis of GFAP and neuN from **a**. Data presented as mean ± SD, $n = 3$ each group; $^*P < 0.05$

Different energy densities were chosen to screen for the optimal parameters for cell proliferation. Combined with the literature and the experimental results, on the one hand, the proliferation and differentiation have certain competitive inhibition. On the other hand, a high dose of energy density produces a high photothermal effect, which has a killing effect on the differentiated nerve cells and affects the final cell differentiation results. Therefore, the energy density of 6 J/cm^2 was selected.

Our studies revealed significant morphological changes in hUC-MSCs at 48 h was after induction. Irradiation with an 808-nm laser by itself or combined with CSF treatment resulted in the most significant morphological changes. Polygonal branching and reduction in triangular morphology were observed. This indicated that the hUC-MSCs may be differentiating into neural cells. Nerve growth factor regulates the microenvironment of cells and promotes neural differentiation of hUC-MSCs [27]. CSF contains nerve growth factors that promote neural differentiation including bFGF, EGF, BDNF, and GDNF. CSF-mediated differentiation induction is similar to physiological induction with neurotrophic factors [21]. Chemical inducers can significantly increase the efficiency of neural differentiation in MSCs, but their toxicity limits continued development [15]. The combination of chemical inducers and neurotrophic factors can promote the differentiation of MSCs into nerve cells [28]. Therefore, this was the reason why that was selected as positive control groups to verify the direction and efficiency of photobiomodulation on neural differentiation in western blot.

We found that nestin located at the cytoplasm was highly expressed in the cells irradiated with an 808-nm laser at 24 h after induction. Meanwhile, the cells showed a triangular distribution, which was consistent with the morphological observations. Nestin expression in the 808-nm laser group and the 808-nm combined with CSF group was positive, and the cells exhibited a slender morphology at 72 h after induction. However, nestin showed a triangular distribution in the 635-nm laser combined with CSF group at the same time point. Because GFAP and neuN proteins have low fluorescence sensitivity, the results were not obvious in immunofluorescence. Due to the large number of experimental groups, the western blot was divided into two gels. The expression of GFAP in the 808-nm laser combined with inducer group was higher than the positive control groups at 24 h after induction. The expression of neuN in CSF group and the 808-nm laser combined iCSF group was higher than positive control groups, suggesting that the hUC-MSCs were beginning to differentiate into neurons. The morphology of cells shows the triangulation or multipolarity (Fig. 3b) and the high expression of nestin/GFAP/neuN neuronal marker protein after induction(Figs. 4b and 5) were sufficient to demonstrate that the 808-nm combined inducer can effectively promote the differentiation of hUC-MSCs. Compared with other proteins, the nestin protein has a larger molecular weight, so it showed no protein band in the western blot.

Low-level laser combined with neurotrophic factors was superior to the combined effect of chemical inducers and shortened the time of stem cell differentiation. During 24 h of pre-induction, photobiomodulation was relatively mild and the inducer played a major role in the differentiation of stem cells into glial cells increasing the expression of GFAP. This effect has been confirmed in several previous studies [16, 29, 30]. With the accumulation of photobiomodulation, multi-level signaling pathways are activated. Activation of signaling coupled with the effect inducers, hUC-MSCs differentiate into neurons. Further studies are needed to understand the underlying mechanisms.

In our study, we combined photobiomodulation and CSF treatments to trigger neural differentiation in stem cells. We achieved increased cell activity and high efficiency of neural differentiation. Photobiomodulation does not produce irreversible damage to cells and can be combined with other inducers. Neural differentiation was achieved in a relatively short time. Further studies are required to optimize the induction time and study the signaling pathways associated with neural cell differentiation of stem cells. The combined effect of photobiomodulation and chemical inducers need to further be studied.

Conclusion

The combined effect of photobiomodulation and biological inducer can improve the efficiency of neural differentiation in MSCs, and the effect of 808 nm is more effective in neural differentiation of hUC-MSCs especially.

Funding This work has been funded by the National Natural Science Foundation of China (Grant Nos. 61705164 and 81801240).

Compliance with ethical standards

All clinical procedures followed the protocols approved by the ethical committee. All participants provided their written consents for the current study.

Conflict of interests The authors declare that they have no conflict of interest.

References

1. Sugimura R, Jha DK, Han A (2017) Haematopoietic stem and progenitor cells from human pluripotent stem cells. Nature 545: 432–438
2. Fisher SA, Doree C, Mathur A (2017) Cochrane corner: stem cell therapy for chronic ischaemic heart disease and congestive heart failure. Heart 104:8–10
3. Jackson WM, Nesti LJ, Tuan RS (2016) Mesenchymal stem cell therapy for attenuation of scar formation during wound healing. China Med Her 3:1–9

4. Mead B, Logan A, Berry M (2017) Concise review: dental pulp stem cells: a novel cell therapy for retinal and central nervous system repair. Stem Cells 35:61
5. Wei L, Wei ZZ, Jiang MQ (2017) Stem cell transplantation therapy for multifaceted therapeutic benefits after stroke. Prog Neurobiol 157: 49–78
6. Maas AI, Stocchetti N, Bullock R (2008) Moderate and severe traumatic brain injury in adults. Lancet Neurol 7:728
7. Rhee KJ, Lee JI, Eom YW (2015) Mesenchymal stem cell-mediated effects of tumor support or suppression. Int J Mol Sci 16:30015–30033
8. Marks PW, Witten CM, Califf RM (2017) Clarifying stem-cell therapy's benefits and risks. N Engl J Med 376:1007
9. Cui YB, Ma SS, Zhang CY (2017) Human umbilical cord mesenchymal stem cells transplantation improves cognitive function in Alzheimer's disease mice by decreasing oxidative stress and promoting hippocampal neurogenesis. Behav Brain Res 320:291–301
10. Marsh SE, Blurtonjones M (2017) Neural stem cell therapy for neurodegenerative disorders: the role of neurotrophic support. Neurochem Int 106:94–100
11. Zhang JJ, Zhu JJ, Hu YB (2017) Transplantation of bFGF-expressing neural stem cells promotes cell migration and functional recovery in rat brain after transient ischemic stroke. Oncotarget 8:102067–102077
12. Li C, Che LH, Shi L (2017) Suppression of basic fibroblast growth factor expression by antisense oligonucleotides inhibits neural stem cell proliferation and differentiation in rat models with focal cerebral infarction. J Cell Biochem 118:3875–3882
13. Zhou Y, Wang Y, Olson J (2017) Heparin-binding EGF-like growth factor promotes neuronal nitric oxide synthase expression and protects the enteric nervous system after necrotizing enterocolitis. Pediatr Res 82:490
14. Robinson J, Lu P (2017) Optimization of trophic support for neural stem cell grafts in sites of spinal cord injury. Exp Neurol 291:87–97
15. Zhu G, Zhou X, Zhou J (2003) BM-MSC culture and induction into neurons. Acta Acad Med Nanjing 23:100–102
16. Pandya H, Shen MJ, Ichikawa DM (2017) Differentiation of human and murine induced pluripotent stem cells to microglia-like cells. Nat Neurosci 20:753–759
17. Rochette-Egly C (2015) Retinoic acid signaling and mouse embryonic stem cell differentiation: cross talk between genomic and non-genomic effects of RA. Biochim Biophys Acta Mol Cell Biol Lipids 1851:66–75
18. Zecha JA, Raberdurlacher JE, Nair RG (2016) Low-level laser therapy/photobiomodulation in the management of side effects of chemoradiation therapy in head and neck cancer: part 2: proposed applications and treatment protocols. Support Care Cancer 24:2793–2805
19. Hentschke VS, Jaenisch RB, Schmeing LA (2013) Low-level laser therapy improves the inflammatory profile of rats with heart failure. Lasers Med Sci 28:1007–1016
20. Iaccarino HF, Singer AC, Martorell AJ (2016) Gamma frequency entrainment attenuates amyloid load and modifies microglia. Nature 540:230
21. Pillai SK, Pond SL, Liu Y (2017) Genetic attributes of cerebrospinal fluid-derived HIV-1 env. Brain 129:1872–1883
22. Mikami R, Mizutani K, Aoki A (2017) Low-level ultrahigh-frequency and ultrashort-pulse blue laser irradiation enhances osteoblast extracellular calcification by upregulating proliferation and differentiation via transient receptor potential vanilloid 1. Lasers Surg Med 50:340–352
23. Shingyochi Y, Kanazawa S, Tajima S (2017) A low-level carbon dioxide laser promotes fibroblast proliferation and migration through activation of Akt, ERK, and JNK. PLoS One 12:e0168937
24. Fekrazad R, Asefi S, Allahdadi M (2016) Effect of Photobiomodulation on mesenchymal stem cells. Photomed Laser Surg 34:533–542
25. Soleimani M, Abbasnia E, Fathi M (2012) The effects of low-level laser irradiation on differentiation and proliferation of human bone marrow mesenchymal stem cells into neurons and osteoblasts–an in vitro study. Lasers Med Sci 27:423–430
26. Peng F, Wu H, Zheng Y (2012) The effect of noncoherent red light irradiation on proliferation and osteogenic differentiation of bone marrow mesenchymal stem cells. Lasers Med Sci 27:645–653
27. Wang J, Ding F, Gu Y (2009) Bone marrow mesenchymal stem cells promote cell proliferation and neurotrophic function of Schwann cells in vitro and in vivo. Brain Res 1262:7–15
28. Zhou ZG, Li ZZ, Lin YX (2015) Differentiation of mesenchymal stem cells derived from human umbilical cord. Chinese J Pathophysiol 2:229–233
29. Mahay D, Terenghi G, Shawcross S (2008) Growth factors in mesenchymal stem cells following glial-cell differentiation. Biotechnol Appl Biochem 51:167–176
30. Haratizadeh S, Nazm MB, Darabi S (2017) Condition medium of cerebrospinal fluid and retinoic acid induces the transdifferentiation of human dental pulp stem cells into neuroglia and neural like cells. Anat Cell Biol 50:107